Journal of Applied Electrochemistry (2006) 36:173–178
DOI 10.1007/s10800-005-9050-6

Potentiometric SO_2 gas sensor based on a thick film of Ca^{2+} ion conducting solid electrolyte

L. WANG and R.V. KUMAR*
Department of Materials Science and Metallurgy, University of Cambridge, Cambridge, CB2 3QZ, UK
*(*author for correspondence, Tel.: +00441223334327; fax: +00441223334567; e-mail: rvk10@cam.ac.uk)*

Received 19 September 2003; accepted in revised form 16 August 2005

Key words: Ca^{2+} conductor, SO_2 sensor, solid electrolyte, thick film

Abstract

A planar miniaturized SO_2 sensor based upon a thick film of Ca^{2+} ion conductor-$CaO{\cdot}0.6MgO{\cdot}6Al_2O_3$ (CMA) with a Na_2SO_4 auxiliary electrode and a Pt/O_2 reference electrode was fabricated and tested. The thick film was fabricated by screen-printing CMA ink on an alumina substrate and then fired at 1823 K. The solid electrolyte was interfaced with a sodium sulphate auxiliary phase containing Pt paste and the sensor showed a good SO_2 response at 873–1073 K. The electromotive force (emf) values obtained were linearly dependent upon the logarithm values of SO_2 concentration in a range of 10–500 ppm. Both the electrodes were exposed to the same test gas thus eliminating the need to separate the electrode chambers.

1. Introduction

Solid state electrochemical sensors for SO_2 have been widely researched. In the early stages, SO_2 sensors using alkali-metal sulphates, such as K_2SO_4 [1, 2], Na_2SO_4-I [3] or Li_2SO_4 [4, 5] as electrolytes with a gaseous or a solid reference electrode were developed. In recent years, practical devices have been fabricated using Nasicon [6, 7], Na–β-Al_2O_3 [8–10] and YSZ [11] with an auxiliary reference based upon sodium sulphate. These sensors are commonly produced as bulk devices. There is a new trend towards miniaturization by the application of thick or thin film technology and micromachining. This makes it possible to integrate sensors with microelectronic circuitry, to combine other sensors into multi-sensors arrays and to manufacture using mass production methods.

Recently Eastman et al. [12] have developed SO_2 sensors based on Li_2SO_4–Ag_2SO_4 electrolyte by both thin film and thick film technology. Reliable and reproducible results are reported for the sensor operating continuously for 4 months. Since their sensor required the separation of the reference electrode chamber from the working electrode chamber it was difficult to fully miniaturize the sensor. Currie et al. [13] have fabricated SO_2 sensors based on sputtered $Na_2SO_4+BaSO_4+Ag_2SO_4$ as a thin film electrolyte with a silver reference electrode. The electrolytic thin film covered both the Ag reference electrode and a Pt working electrode. Sufficient sensitivity, selectivity and response time was reported. However, as the silver reference is exposed to SO_2 during operation, this was found to reduce the lifetime of the reference electrode. The operating temperature is limited by the liquidus temperature of the electrolyte.

Ca–β''-Al_2O_3, which shares the structural features of Na–β''-Al_2O_3 is a known ionic conductor of calcium ions. Dunn and Farrington have reported high Ca^{2+} ionic conductivity in Ca–β''-Al_2O_3, which was prepared from Na–β''-Al_2O_3 by an ion exchange process [14, 15]. Kirchenerova et al. [16] have found that ion-exchanged Ca–β''-Al_2O_3 is thermally unstable at elevated temperature which transforms to calcium magnetoplumbite which has a structure similar to that of the Na–β''-Al_2O_3. Kumar et al. [17] have investigated the preparation of Ca–β''-Al_2O_3 type of electrolyte by the solid-state ceramic route and optimal conditions for preparation were obtained. The composition of this solid electrolyte is nominally $CaO{\cdot}0.6MgO{\cdot}6Al_2O_3$ (CMA) and has a magnetoplumbite type of structure. At temperatures higher than 873 K the material has sufficiently high Ca^{2+} ionic conductivity for use in sensors [18]. Further Kumar et al. [19] have studied the thermodynamic stability of CMA by determination of the activity of CaO. Such a material has been successfully employed in galvanic cells for measurement of thermodynamic data of the CaO–Al_2O_3 system [17] as well as the Ca–Pb system [20]. Gog et al. [21] used

$CaSO_4$ as the auxiliary phase in contact with Ca–β''-Al_2O_3 solid electrolyte to develop SO_2 sensors. Recently the present authors have successfully fabricated a bulk SO_2 sensor with an open reference electrode based on this electrolyte [22]. The purpose of this work was to prepare a planar sensor by means of the widely used thick film technology of screen printing [23] and to investigate the sensor characteristics.

2. Theory

The measuring electrode was made of Na_2SO_4 mixed with platinum metal paste. The reference electrode was made of Pt which allows reversible exchange of oxygen in the gas phase with Ca^{2+} ion in the electrolyte.

The working cell can be depicted as follows:

$$\begin{aligned}&SO_2, O_2, Pt|CaO \cdot 0.6MgO \cdot 6Al_2O_3\\&\quad \text{film}|Na_2SO_4|Pt, O_2, SO_2\end{aligned} \tag{14}$$

Both electrodes are exposed to the same test gas. The following reaction scheme is proposed for the system.

Firstly SO_2 in the gas mixture is catalytically converted into SO_3 *in situ* when the gas passes through the porous Pt layer on the surface of the auxiliary electrode by following reaction:

$$SO_2 + 1/2O_2 = SO_3 \tag{1}$$

It has been shown previously (11) that:

$$P_{SO_3} = P_{SO_2}\frac{KP_{O_2}^{1/2}}{1 + KP_{O_2}^{1/2}} \tag{2}$$

where K is equilibrium constant for above reaction (1).

The cell reactions are identical to those proposed for bulk sensors and reported elsewhere [22].

At the working electrode:

$$2Na^+ + 1/2O_2 + SO_3 + 2e^- = Na_2SO_4 \tag{3}$$

and at the reference electrode:

$$\text{CaO [in CMA]} = 1/2O_2 + 2e^- + Ca^{2+} \tag{4}$$

To establish an electrochemical chain within the cell, an ionic bridge between CMA and Na_2SO_4 must exist. So the operation of the sensor presupposes an exchange reaction at the surface of the CMA solid electrolyte with the Na_2SO_4 auxiliary phase, driven by the formation of a metastable $CaSO_4$ phase within the Na_2SO_4. The exchange reaction at the auxiliary phase/solid electrolyte interface can be expressed as:

$$Ca^{2+} + Na_2SO_4 = CaSO_4[\text{in } Na_2SO_4] + 2Na^+ \tag{5}$$

$$\text{Overall: CaO [in CMA]} + SO_3 = CaSO_4[\text{in}Na_2SO_4] \tag{6}$$

Thus the emf of the sensor is related to the partial pressure of SO_3 in the gas mixture by the expression

$$E = -\frac{\Delta G^0}{2F} + \frac{2.303RT}{2F}\log\left(\frac{P_{SO_3}a_{CaO}}{a_{CaSO_4}}\right) \tag{7}$$

Combining Equations (2) and (7), the relationship between emf and SO_2 partial pressure can be expressed as:

$$\begin{aligned}\text{EMF} = &-\frac{\Delta G^0}{2F} + \frac{2.303RT}{2F}\log\left(\frac{KP_{O_2}^{1/2}}{1 + KP_{O_2}^{1/2}}\right)\\&+\left(\frac{2.303RT}{2F}\right)\log P_{SO_2} + \frac{2.303RT}{2F}\log\left(\frac{a_{CaO}}{a_{CaSO_4}}\right)\end{aligned} \tag{8}$$

Thus:

$$E = a + b\log P_{SO_2} \tag{9}$$

where $a = -\frac{\Delta G^0}{2F} + \frac{2.303RT}{2F}\log\left(\frac{KP_{O_2}^{1/2}}{1+KP_{O_2}^{1/2}}\right) + \frac{2.303RT}{2F} \times \log\left(\frac{a_{CaO}}{a_{CaSO_4}}\right)$ and $b = \frac{2.303RT}{2F}$; ΔG^0 is the standard free energy of reaction (6); R, T and F have their usual meaning; a_{CaO} and a_{CaSO_4} are the activities of CaO in CMA and $CaSO_4$ in Na_2SO_4, respectively. The overall emf is independent of oxygen partial pressure for a SO_3 sensor, because the oxygen is involved in both electrode reactions and is thus cancelled out. The emf is dependent on the oxygen partial pressure for a SO_2 sensor through the SO_2/SO_3 equilibrium.

In the operation of such a SO_2 sensor, it is not only important that the electrolyte/Pt interface is sensitive only to O_2, but also that it is chemically stable when exposed to SO_2/SO_3 atmosphere. In other words, the free energy change (ΔG) for the following reaction must be positive

$$\text{CaO (in CMA)} + SO_3 = CaSO_4 \tag{10}$$

$$\Delta G = \Delta G^0 - 2.303RT\log P_{SO_3}a_{CaO} \tag{11}$$

Using literature data on the activity of CaO in the solid electrolyte [20] and thermodynamic data of compounds, the authors [22] have shown that CMA is stable and $CaSO_4$ will not form on the surface of the electrolyte at operating temperatures of 873–1073 K over a wide range of SO_2/SO_3 concentration. These calculations have also shown that if $CaSO_4$ is used as an auxiliary phase, there will be a driving force for $CaSO_4$ dissolution into the CMA accompanied by decomposition of the auxiliary phase. This is the main reason for using Na_2SO_4 as the auxiliary phase.

3. Experimental

3.1. *Materials*

$CaO \cdot 0.6MgO \cdot 6Al_2O_3$ (CMA) powder was prepared using the conventional calcination-sintering route [17, 22] from precursors of magnesium oxide, calcium carbonate and alumina. These powders were mixed according to the required ratio (CaO:MgO:Al_2O_3 = 1:0.6:6) and ball-milled in acetone for a total of 12 h. The powder slurry was dried and then placed in an alumina crucible and calcined at 1173 K for 6 h in air. The calcined powder was returned to the ball mill and re-milled for a further 24 h. The slurry was then dried and re-sieved. The planar sensor design was based on screen printing the electrolyte on to the substrate followed by an *in situ* firing step. A screen printing formulation was developed. The ink formulation was made up by mixing 50 g CMA powder, 6.6 g ethylcellulose, 2.9 g furoric acid and 50 g butylcarbitol acetate. The powder and butylcarbitol acetate were mixed together to form a slurry. The other two components were added slowly and mixed to ensure complete dispersion. The slurry diluted with additions of acetone was milled for a further 24 h before being poured into a large Pyrex basin ready for screen printing.

Commercially available alumina tiles 50×50 mm^2 and approximately 0.5 mm thick were chosen as the substrate material. Each tile was laser scribed to allow several individual sensors to be printed on one large tile.

Screen printing was performed using a DEK 240 table mounted screen printer. The thick film was then fired at 1823 K for 1 h in order to densify the electrolyte layer before attaching the electrodes.

3.2. *Preparation of the sensor*

For SO_2 sensors, the reference and sensing electrodes were fabricated by painting commercial Pt paste on the designated regions and annealed at 1173 K for 30 min. A porous film of $Pt + Na_2SO_4$ auxiliary electrode was deposited on the Pt sensing electrode by painting a paste of $Pt + Na_2SO_4$ followed by melting (at 1173 K) and quenching. The structure of the sensor is shown in Figure 1.

3.3. *Experimental procedure*

{PRIVATE "TYPE=PICT; ALT="} The SO_2 sensors were tested in controlled conditions at different SO_2 contents and operating temperatures. Measurements were carried out in a conventional gas-flow apparatus equipped with a heating furnace. Premixed sample gases, which were prepared by diluting a parent gas (5000 ppm SO_2 in air/N_2), with synthetic air or Ar using gas blender and were allowed to flow through the quartz tube where the sensor was positioned at a controlled flow rate of typically 200 $cm^3\ min^{-1}$. The SO_2 concentration in gas mixture was varied from 10 to 500 ppm. Operating temperatures from 873 to 1073 K were investigated. The partial pressure of oxygen in the gas was independently controlled. Electromotive forces (emfs) were measured with a high impedance electrometer ($> 10^{12}$ ohm) and the data transferred to a PC based data collecting system (Pico ADC-16).

4. Results and discussions

A typical emf response to stepwise increase in the SO_2 concentration from 1 to 500 ppm for a planar SO_2 sensor at a temperature of 961 K and at $P_{O_2} = 0.21$ atm is shown in Figure 2. Emf signals change rapidly, typically in less than 60 s, in response to changes in SO_2 concentration, although it took longer ($\sim$500 s) to achieve 90% of the steady state emf values. Variation of the sensor emf with SO_2 concentration in the gas mixture at 961 K is presented in Figure 3. The relationship between emf and the logarithm value of the partial pressure of SO_2 at a fixed P_{O_2} value is found to be linear over the whole concentration range tested.

The slope of the response curve calculated from the experimental data is 74.5 mV $decade^{-1}$ at 961 K. From the slope, using the Nernst equation, the number of electron transferred in the electrochemical reactions is calculated to be 2.5 rather than the proposed 2.0. This difference may be partially attributed to the lack of emf stabilization, especially at the low concentration end, thus resulting in a higher slope than predicted.

Figure 4 gives a typical emf response to stepwise decrease in the O_2 concentration from 0.21 atm to about

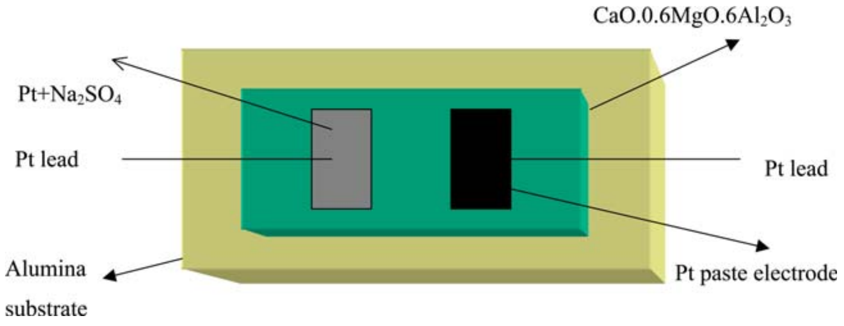

Fig. 1. A schematic diagram of planar miniaturized SO_2 sensor device using CMA solid electrolyte film with a Na_2SO_4 auxiliary electrode.

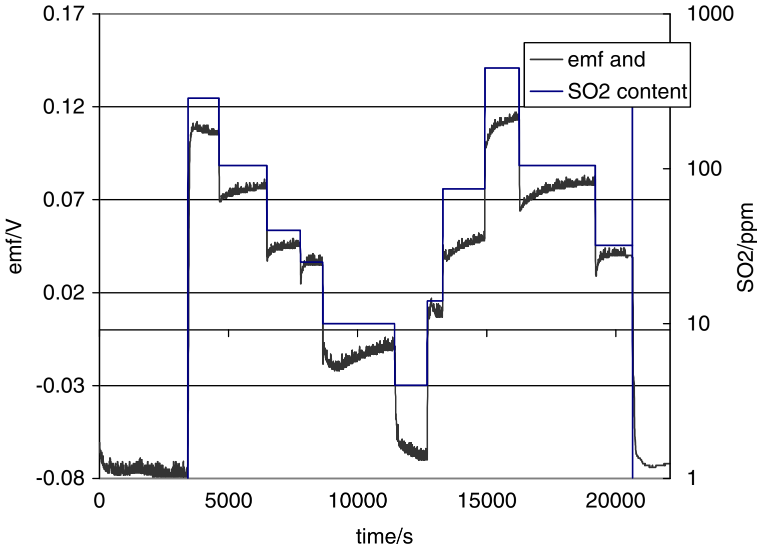

Fig. 2. Emf response to various SO_2 content (at $P_{O_2} = 0.21$ atm) at 961 K.

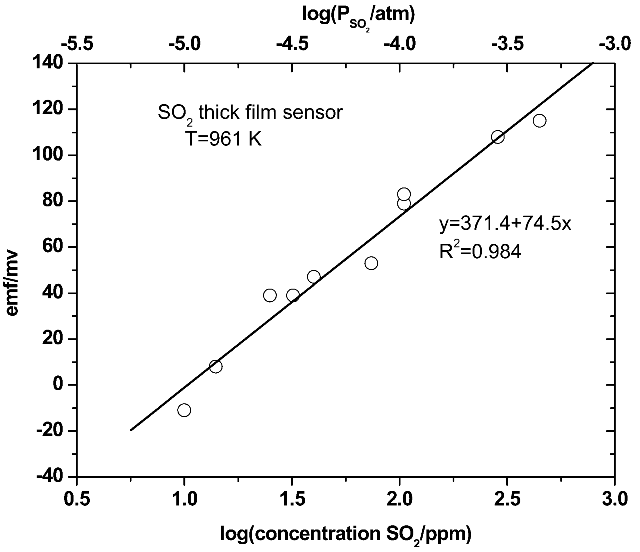

Fig. 3. Emf response as a function of the logarithm of SO_2 partial pressure, measured at 961 K.

200 ppm for a planar SO_2 sensor at a temperature of 962 K and at $P_{SO_2} = 72$ ppm. The emf of the cell decreased as P_{O_2} was decreased.

Figure 5 presents emf changes with variation of O_2 concentration in the gas mixture from 200 ppm to 0.21 atm with SO_2 fixed at 74 ppm. The emf linearly increased with increased oxygen partial pressure in the first part. The linear equation can be expressed as $E = -34.7 + 546.2P_{O_2}$. At high oxygen partial pressure, the emf values begin to plateau to a constant value. At a given SO_2 concentration when the oxygen concentration is low, the conversion rate of SO_2 to SO_3 is strongly dependent on the oxygen partial pressure. When the oxygen partial pressure is high, its effect on conversion becomes weak, which is in agreement with Equation (8).

In order to evaluate the effect of the temperature on emf, the sensor was tested at different fixed temperatures. Figure 6 shows the dependence of emf response on the logarithm of SO_2 concentration ($\log P_{SO_2}$), measured at 937, 961 and 1024 K. The emf response of the sensor was linear, with positive slope, to the logarithm of SO_2 concentration ($\log P_{SO_2}$) at each temperature. The emf as a function of the content of SO_2 in the gas mixture is given by:

$$E_1 = 403 + 77.3 \log P_{SO_2} \quad (937\,\mathrm{K}) \tag{12}$$

$$E_2 = 371 + 74.5 \log P_{SO_2} \quad (961\,\mathrm{K}) \tag{13}$$

$$E_3 = 421 + 86.4 \log P_{SO_2} \quad (1024\,\mathrm{K}) \tag{14}$$

The calculated number of transferred electrons, derived from the Nernstian equation as applied to the best linear fit, are 2.3, 2.5 and 2.4, at temperatures of 937, 961 and 1024 K, respectively. The deviation of transferred electron number from two can be explained by looking at the scatter of data around the fit line. If the scattered data is ignored, the calculated number of transferred electrons approaches two. The scatter may be related to lack of complete equilibrium between $SO_2/O_2/SO_3$ on the Pt/Na_2SO_4 surface and changes in a_{CaO} due to surface exchange reactions.

Both the bulk and the thick film SO_2 sensors based on the CMA/Na_2SO_4 system display similar sensing properties with respect to response mechanism, response time and the influence of O_2 partial pressure. However, for a given gas composition the following differences have been observed. The emf of the thick film sensor is lower than those of a bulk sensor; the sensitivity of bulk sensor is higher than that of film sensor and the results were more scattered with the thick film sensor. These may be attributed to variations in a_{CaO} in solid electrolyte film due to surface exchange reactions and chemical reactions between alumina substrate and electrolyte film during preparation and also to lack of

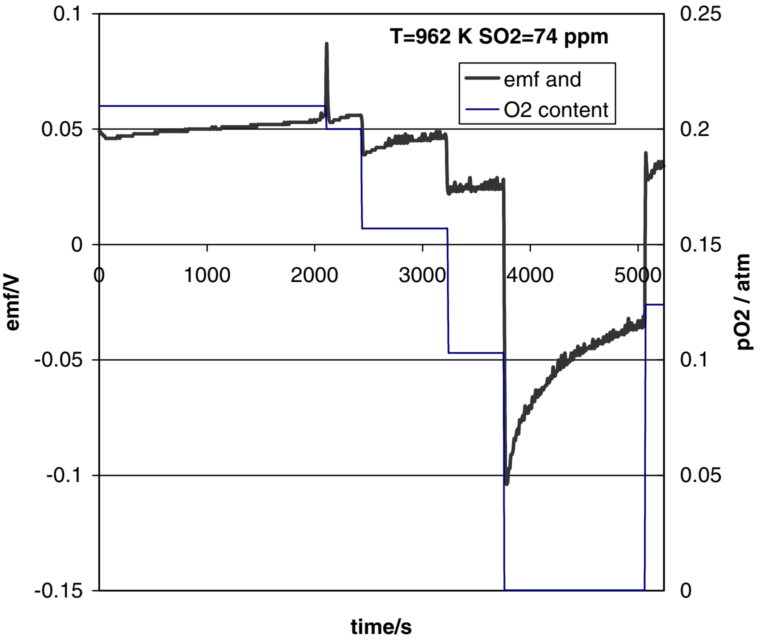

Fig. 4. Emf response to various O_2 content (at $P_{SO_2} = 74$ ppm) at 962 K.

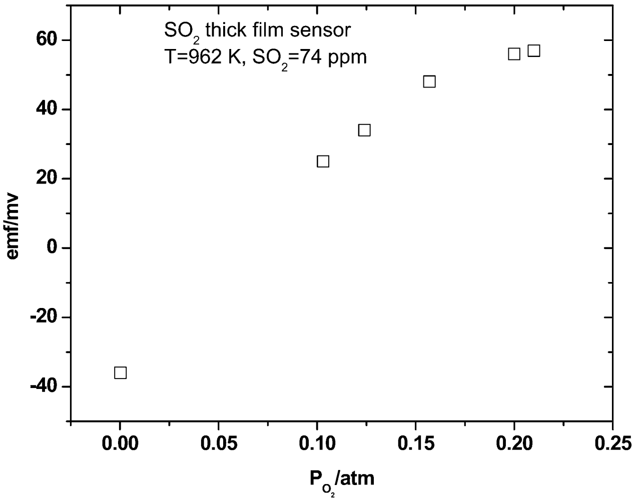

Fig. 5. Emf response as a function of O_2 partial pressure at SO_2 fixed at 74 ppm, measured at 962 K.

complete equilibrium between $SO_2/O_2/SO_3$ on the Pt/Na_2SO_4 surface in film sensor.

5. Conclusion

$CaO \cdot 0.6MgO \cdot 6Al_2O_3$ thick film solid electrolyte is fabricated by screen printing technology on an alumina substrate. A planar SO_2 sensor based on this film with a Na_2SO_4 auxiliary electrode exhibits a satisfactory performance for detecting SO_2 in the concentration range of 10–500 ppm. The measured emf of the sensor was found to be a linear function of logarithm of partial pressure of SO_2 over the whole range of concentration at 873–1073 K, although some deviation from Nernstian slope exists. The sensor allows seal-free open cell arrangement with a single electrode chamber, and the results are consistent with the assumption that the CMA/Pt interface is sensitive to oxygen, while the Na_2SO_4/Pt auxiliary is simultaneously sensitive to SO_2 and O_2.

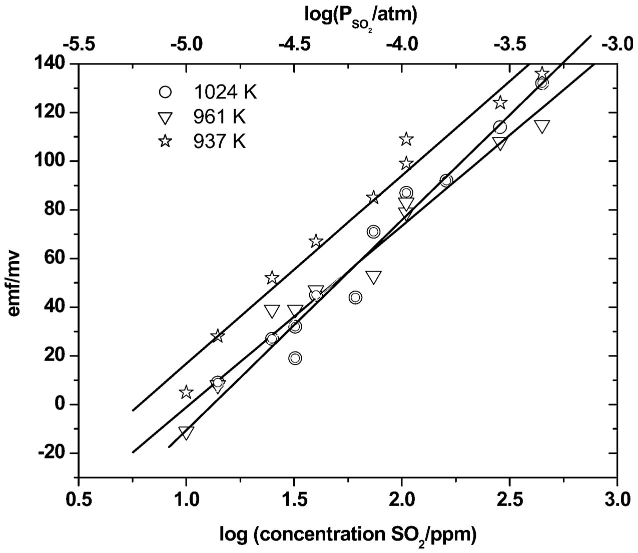

Fig. 6. Emf response as a function of the logarithm of SO_2 partial pressure measured at 937, 961 and 1024 K.

Acknowledgement

The financial support of EPSRC for this project is gratefully acknowledged.

References

1. M. Gauthier, A. Chamberland, A. Belanger and M. Poirier, *J. Electrochem. Soc.* **124** (1977) 1584.

2. M. Gauthier, R. Bellemare and A. Belanger, *J. Electrochem. Soc.* **128** (1981) 371.
3. K.T. Jacob and D.B. Rao, *J. Electrochem. Soc.* **126** (1979) 1842.
4. Q. Liu and W.L. Worrell, US Patent No. 4,622,105 (1986).
5. W.L. Worrell and Q. Liu, *J. Electrochem. Soc.* **168** (1984) 355.
6. T. Maruyama, Y. Saito, Y. Matsumoto and Y. Yano, *Solid State Ionics* **17** (1985) 281.
7. G.M. Kale, L. Wang and Y.R. Hong, *Solid State Ionics* **161** (2003) 155.
8. R. Akila and K.T. Jacob, *J. Appl. Electrochem.* **18** (1988) 245.
9. R. Akila and K.T. Jacob, *Sensor Actuator* **16** (1989) 311.
10. G. Rog, A. Kozlowka-Rog and K. Zakula, *J. Appl. Electrochem.* **21** (1991) 308.
11. R.V. Kumar, *J. Alloy Compound* **250** (1997) 501.
12. C.D. Eastman and T.H. Etsell, *Solid State Ionics* **136/137** (1992) 639.
13. J.F. Currie, A. Essalik and J.-C. Marusic, *Sensor Actuator B* **59** (1999) 235.
14. B. Dunn and G.C. Farrington, *Mat. Res. Bull.* **15** (1980) 1773.
15. J.T. White and D.J. Fray, *Solid State Ionics* **17** (1985) 1.
16. J. Kirchnerova, A. Petric, C.W. Bale and A.D. Pelton, *Mat. Res. Bull.* **26** (1991) 527.
17. R.V. Kumar and D.A.R. Kay, *Metall. Trans. B* **16** (1985) 107.
18. Y. Hong, D. Hong, Y. Peng, L. Li and S. Wei, *Solid State Ionics* **25** (1987) 301.
19. R.V. Kumar and D.A.R. Kay, *Metall. Trans. B* **16** (1985) 295.
20. D.J. Fray and R.V. Kumar, *Scand. J. Metall.* **22** (1993) 266.
21. G. Rog, A. Kozlowska-Rog, K. Zakula, W. Bogusz and W. Pycior, *J. Appl. Electrochem.* **21** (1991) 313.
22. L. Wang and R.V. Kumar, Mater. Sci. Technol. **19** (2003) 1478.
23. L. Wang and R.V. Kumar, Solid State Ionics **158** (2003) 309.